Eur. Radiol. 10, 188–194 (2000)

European
Radiology

Original article

Treatment of VX2 liver tumor in rabbits with "wet" electrode mediated radio-frequency ablation

Y. Miao[1, 4], Y. Ni[1], S. Mulier[2], J. Yu[3], I. De Wever[2], F. Penninckx[2], A. L. Baert[1], G. Marchal[1]

[1] Department of Radiology, University Hospitals, Herestraat 49, Gasthuisberg, B-3000 Leuven, Belgium
[2] Department of Surgery, University Hospitals, Herestraat 49, Gasthuisberg, B-3000 Leuven, Belgium
[3] Department of Pathology, University Hospitals, Herestraat 49, Gasthuisberg, B-3000 Leuven, Belgium
[4] Department of Abdominal Surgery, Nanjing Medical University, Nanjing, China

Received: 14 January 1999; Revised: 9 April 1999; Accepted: 17 June 1999

Abstract. Radio-frequency ablation (RFA) has been considered as an alternative therapy for liver tumors. A "wet" electrode with interstitial infusion of hypertonic saline was tested for the RFA of liver tumor in rabbits. Seventy-eight liver tumors (∅ 1.5 to 3.0 cm) were induced in 41 rabbits by VX2 carcinoma implantation. Fifty-one tumors in 27 rabbits were treated with RFA. Under laparotomy, the RF energy was delivered while 5% saline was infused through the electrode into the tumor at 1 ml/min. Six rabbits with 12 tumors were treated with only intratumoral 5% saline infusion without RFA. Another 8 rabbits with 15 tumors received sham operation as untreated controls. The efficacy of the therapy was evaluated with survival rate, MRI, microangiography, and histopathology. In the RFA group, 6 rabbits survived longer than 6 months (absolute eradication rate 22.2%); 12 rabbits were found free of viable tumor at the moment when they were sacrificed (relative eradication rate 44.4%); 9 rabbits showed local tumor relapse and/or lung metastasis 2–10 weeks after ablation (recurrent rate 33.3%). In control groups of saline infusion and sham operation, all 14 rabbits died within 3 months (mortality rate 100%). Three-month survival rates between RFA group and control groups were significantly different ($p < 0.05$). Findings of MRI, microangiography, and histology supported these outcomes. Radical treatment of liver malignancy in rabbits is possible with the present modified RFA technique. Its clinical usefulness has to be further proven.

Key words: Liver – Interventional procedure – Neoplasms – Radio-frequency ablation

Introduction

Although surgical resection is still considered as a primary option for the treatment of liver malignancies [1, 2, 3], less invasive therapies, including intraoperative cryosurgery [4], ethanol injection [5, 6], microwaves [7, 8], interstitial laser therapy [9], focused ultrasound [10, 11], and radio-frequency ablation (RFA) [12, 13, 14, 15, 16, 17, 18, 19, 20, 21, 22] have been developed as alternatives to conventional surgery. Among these approaches, RFA has shown the greatest potential in recent experimental and clinical research owing to its low invasiveness, simplicity, and favorable cost-effectiveness. Because of technical innovations, such as cooled electrode [15, 16, 17], bipolar electrode [18], and expandable electrode [19], the ablated lesion size has been dramatically increased from several millimeters to several centimeters. Another strategy to enlarge the ablation volume is to infuse 0.9% saline into the tissue via a hollow electrode, where the infused saline functions as a "liquid electrode" to enhance the RFA capacity [13, 21]. A recent study with excised pork liver has demonstrated that lesion size induced with hypertonic-saline (5%) mediated RFA is significantly larger than that without saline infusion [22]. The present animal experiment was conducted to verify this modified technique in treatment of liver malignant tumors. Rabbits with liver implantation of VX2 carcinoma were used as animal models. To better control the procedure, RFA was performed under laparotomy. The therapeutic effects were compared between animals with RFA, saline infusion alone, and sham operation by periodic follow-up with MRI, postmortem angiography, and histology. The potential of this technique for future clinical application has been discussed.

Correspondence to: Y. Ni

Materials and methods

Tumor model

Forty-one adult male New Zealand rabbits weighing 2–3.0 kg were anesthetized with intramuscular injection of a mixed solution of Ketalar (Katamine Hydrochloride, Parke-Davis N.V. Warner-Lambert Belgium SA) and Ranpun (Xylazine Hydrochloride, Bayer AG, Levekusen, Germany) at 0.5 ml/kg each and laparotomized with a mid-line incision. In order to improve the experimental efficiency, tumor implantation was made in both the left and right liver lobes. A modified technique of liver tumor implantation was adapted from a rat experiment [23]. Briefly, freshly harvested tumor mass from intramuscular growth of VX2 carcinoma was minced into $2 \times 2 \times 2$-mm cubes containing approximately 1.5×10^6 tumor cells. After a small incision on liver capsule, a small pocket in liver parenchyma was made by blunt division and temporary insertion of a piece of gelatin sponge (Spongostan, Ferrosan Co., Soeborj, Denmark). One tumor fragment was placed into each pocket while the sponge had been withdrawn. The liver incision was sealed with tissue-adhesive Histoacryl (B. Braun AG, Melsungen, Germany) and abdominal wall was closed in double layers. The animals were scanned with MRI from 14 days after implantation to monitor tumor growth. VX2 lesions of 1.5–3.0 cm were considered appropriate for RFA. The tumor growth was found in 95% of the implantation sites.

Ablation protocol

The performance of current modified RFA is illustrated in a simplified scheme (Fig. 1) and was described previously [22]. Under the same anesthetic and laparotomy regimes as in tumor implantation, the liver lobe barring VX2 tumor was explored and adjacent organs were protected with gauze pads and plastic plates. Under direct visual inspection, the tumor was inserted with a hollow screw-tip electrode (5 F with one end hole and four side holes of 0.12-mm diameter) which was filled with 5% saline and connected to an infusion pump (Ismatic, Switzerland). A thermocouple (type K, Omega Engineering, Stanford, Conn.) was inserted in contact with the distal electrode to monitor tip temperature. With hypertonic saline (5% NaCl, Baxter N.V., Lessines, Belgium) infusion at 1 ml/min 1 min prior to and during the ablation, RF current (475 ± 20 kHz) was delivered from a generator (Medtronic, San Jose, Calif.). Temperature control mode was set at 90 °C for 4–10 min depending on the size of the tumor. The marginal temperature was monitored by placing an additional thermocouple in liver parenchyma 1.5 cm apart from the edge of the tumor. The ablation was seized when the tumor was seen to be well included in the coagulated bulk (tumor mass plus a safety margin of at least 1.5 cm) and/or when marginal temperature reached above 55 °C. Another session of RFA was performed if the rabbit possessed a second tumor on the other liver lobe. The abdominal incision was closed after the therapy. Altogether 51 VX2 tumors were thus treated in 27 rabbits. Twelve VX2 tumors in 6 rabbits were infused with 10 ml of 5% saline without RFA. Another 8 rabbits carrying 15 tumors underwent sham laparotomy and served as untreated control.

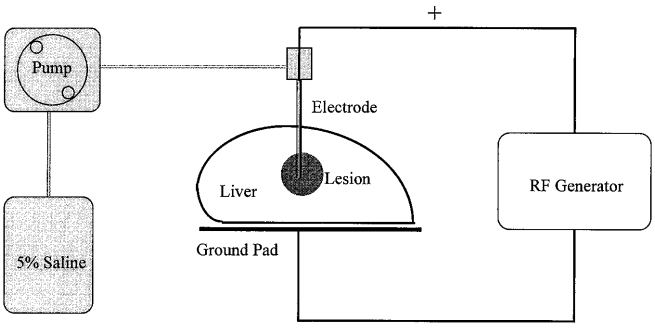

Fig. 1. Illustration of radio-frequency (RF)-ablation with saline infusion

MRI follow-up

Transverse T1- (TR/TE = 450/12 ms) and T2- (TR/TE = 2500/90 ms) weighted spin-echo MRI (slice thickness of 3 mm) was obtained with a knee coil in a 1.5-T Magnetom Vision (Siemens, Erlangen, Germany) to follow the tumor growth after implantation and to monitor the ablation effects periodically at days 0, 1, and 3, weeks 1 and 2, and months 1, 2, 3, and up to 6 post therapy. The diameter of the tumor and RF induced necrotic lesion were measured with the monitor-defined distance function. Local and remote liver tumor relapse, as well as metastasis to the abdominal cavity and lungs, was also detected with MRI.

Postmortem microangiography

As designed, the rabbit was killed at certain time points with intravenous overdose of pentobarbital (Nembutal, Abbott Laboratories, North Chicago, Ill.). Before excision of the liver, the hepatic artery was injected with 50% barium suspension. The magnified hepatic angiography was performed on the excised liver using a clinical mammography unit (Mammomat-2, Siemens, Erlangen, Germany) with Agfa Mannoray MR3-II film (Agfa-Graevert N.V., Brussels, Belgium) at 38 kV and 5.0 mAs.

Histopathologic examination

The liver specimens were suspended in 10% formalin solution for fixation, and then dissected in planes similar to those of MRI, and finally processed with paraffin section and hematoxylin–eosin (HE) staining for light microscopic study. The gross specimens, liver sections, and microscopic views were all photographed for documentation.

Table 1. Summary of radio-frequency (RF) tumor ablation effect

Groups	No. of animals	No. of tumors	Tumor size (mm)[a]	Local growth (%)	Lung metastasis (%)	Eradication rate (%)[b]
RF ablation	27	51	21 ± 7	11	26	67
Saline infusion only	6	12	20 ± 4	100	67	0
Sham operation	8	15	19 ± 4	100	63	0
Total	41	78	21 ± 7	–	–	–

[a] Maximal diameter measured with MRI before operation
[b] Absolute and relative eradication

Evaluation of RFA efficacy

Therapeutic assessment was based on the following criteria: (a) absolute tumor eradication: animals survived longer than 6 months without any evidence of viable tumor; (b) relative tumor eradication: animals killed within 3 months after therapy and found free of viable tumor with MRI, microangiography, and histology; and (c) tumor local recurrence and remote metastasis.

Statistical analysis

The sizes of VX2 tumors in RFA treated, saline-infused, and sham-operated groups were compared before treatment by using unpaired student *t*-test. The mean survival periods of rabbits and lung-metastatic rate were calculated. The values were expressed as the mean ± standard deviation. Between RFA-treated, saline-infused, and untreated groups, 3-month survival rate was compared by using chi-square test. The *p*-values less than 0.05 were considered to be significant. All statistical analyses were performed with computer software Microsoft Excel 7.0 (Microsoft, Seattle, Wash.).

This experiment complied with the current guidelines for use and care of laboratory animals of this institute.

Results

General aspects of the study

All control rabbits and most of the RFA-treated rabbits tolerated well the experimental procedures. After RFA, 3 rabbits were critically ill due to overdose of anesthetics ($n = 2$) and hepatic dysfunction ($n = 1$), as a result of massive liver ablation (> 70 %), and were killed within 3 days after therapy. One rabbit with relative tumor eradication developed a perihepatic abscess.

Tumor ablation effect

As shown in Table 1, the animals in control groups died of end-stage malignancy within 3 months (100 % mortality rate). In RFA group, absolute tumor eradication was achieved in 6 rabbits (22.2 %) which survived longer than 6 months. Relative eradication was found in 12 rabbits (44.4 %), i. e., one rabbit each was found free of viable tumor when killed at days 0, 1, 3, and months 1 and 2; 2 rabbits each at day 7 and week 2; and 3 rabbits at month 3. However, 9 rabbits (33.3 %) suffered from local tumor relapse ($n = 3$, all sized approximately 3 cm with insufficient ablation at the periphery of the tumor due to cooling effect) and/or lung metastasis ($n = 7$). Three-month survival rate of RFA-treated rabbits was significantly higher ($p < 0.01$) than that of saline-infusion-only and untreated rabbits. Before treatment, there was no statistical difference between tumor diameters of RFA-treated (21 ± 7 mm), saline-infusion-only (20 ± 4 mm), and untreated (19 ± 4 mm) groups ($p > 0.05$).

MRI appearance

Without RF ablation, liver implantation of VX2 carcinoma appeared as hypointense spherical nodules on T1-weighted spin-echo images (Fig. 2A). Within 1 week after RFA, tumors remained hypointense relative to the slightly hyperintense ablated peritumoral liver parenchyma on T1-weighted MRI (Fig. 2B). The ablated bulk was frequently demarcated with a hyperintense rim on T1 images. Gradually signal intensities of ablated tumor and adjacent liver were homogenized with hyper- and hypointense signals on T1- (Fig. 2C) and T2- (Fig. 2D) weighted images. Three months or later after ablation, a hypo- or hyperintense layer appeared around the lesion on T1- or T2-weighted images (Fig. 2C, D). Recurrent tumors shared the same imaging features as those before RFA therapy. Lung metastasis could easily be detected with MRI as hyperintense nodules.

Microangiographic findings

VX2 carcinomas in the liver were generally hypervascularized with well-developed hypertrophic and tortuous feeding arteries (Fig. 3A). After RFA, tumors as well as adjacent liver tissue are completely or largely devascularized and show on microangiogram as a barium-filling defect (Figs. 2E, 3C). Relapsed tumors were frequently found to be associated with incompletely destroyed tumoral vessels.

Histopathologic examination

Macroscopically, eradicated tumors appeared as an atrophied mass (Fig. 2F), whereas recurrent tumors showed multinodular growth. At cross section of the le-

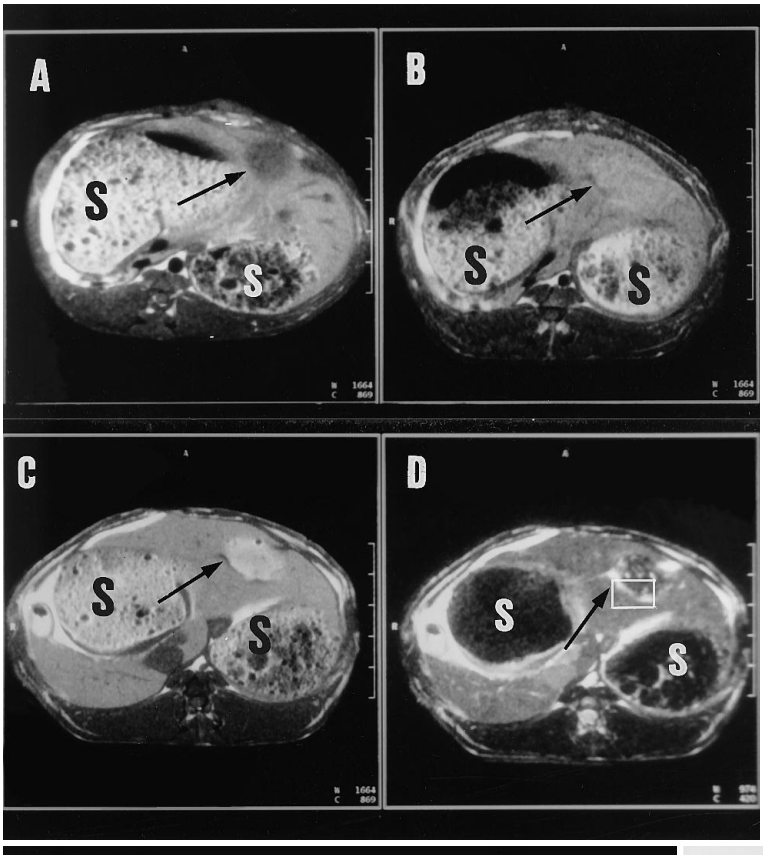

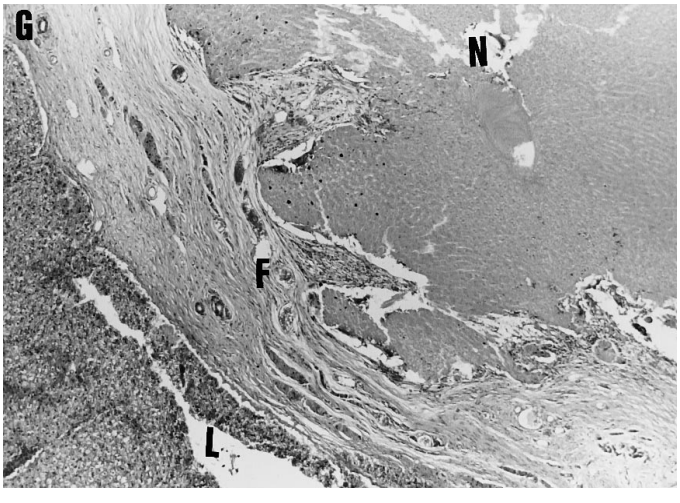

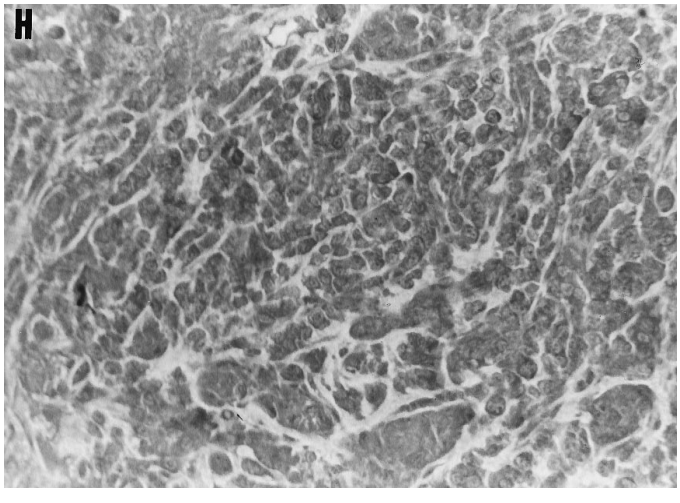

Fig. 2 A–H. Long-term follow-up of VX2 tumor eradication in a rabbit of RF-treated group. **A** Transverse T1-weighted spin-echo (SE) MRI obtained 2 weeks after tumor implantation but before RF ablation displays a hypointense spherical VX2 tumor *(arrow)* approximately 1.5 cm in diameter in the left liver lobe. *S* represents the stomach filled with food. **B** Transverse T1-weighted SE MRI obtained 24 h after RF tumor ablation displays in the left liver lobe a 2 × 3-cm slightly hyperintense lesion *(arrow)* encompassing both the tumor and a safety margin. **C** Transverse T1-weighted SE MRI obtained 3 months after RF tumor ablation displays the hyperintense RF-ablated lesion in the left liver lobe *(arrow)*, which is atrophied (in comparison with **B**) and surrounded with a thin hypointense peripheral layer. **D** Transverse T2-weighted (TR/TE = 2500/90 ms) SE MRI obtained at the same time point as in **C** displays the lesion as a hypointense area surrounded with a hyperintense rim *(arrow)*. The *square* indicates where the microscopy **(G)** was taken. **E** Microangiography of the liver specimen shows void opacity of the tumoral region (contoured with *arrowheads*), a sign of complete destruction of the tumoral vasculature. *Arrow* indicates one of the abruptly truncated tumoral feeding arteries. **F** The corresponding macroscopic photograph of the excised liver shows the RF ablated and atrophied tumor in the left lobe *(arrow)*. **G** Light microscopic view of the boundary of RF-ablated lesion reveals the central eosinophilic coagulation necrosis *(N)*, the peripheral fibrotic scaring tissue *(F)*, and surrounding normal liver tissue *(L)*. The first two components correspond respectively to the hyperintense center and hypointense rim on T1-weighted MRI, or to the hypointense center and hyperintense rim on T2-weighted MRI (hematoxylin and eosin staining, original magnification × 100). **H** Light microscopic view with more powerful magnification displays the central coagulation necrosis of the VX2 tumor as homogenous eosinophilic matrix. Although the VX2 tumor is completely cytolytic after 3 months, the global outline of tumor cell nests can still be recognized. (Hematoxylin and eosin staining, original magnification × 400)

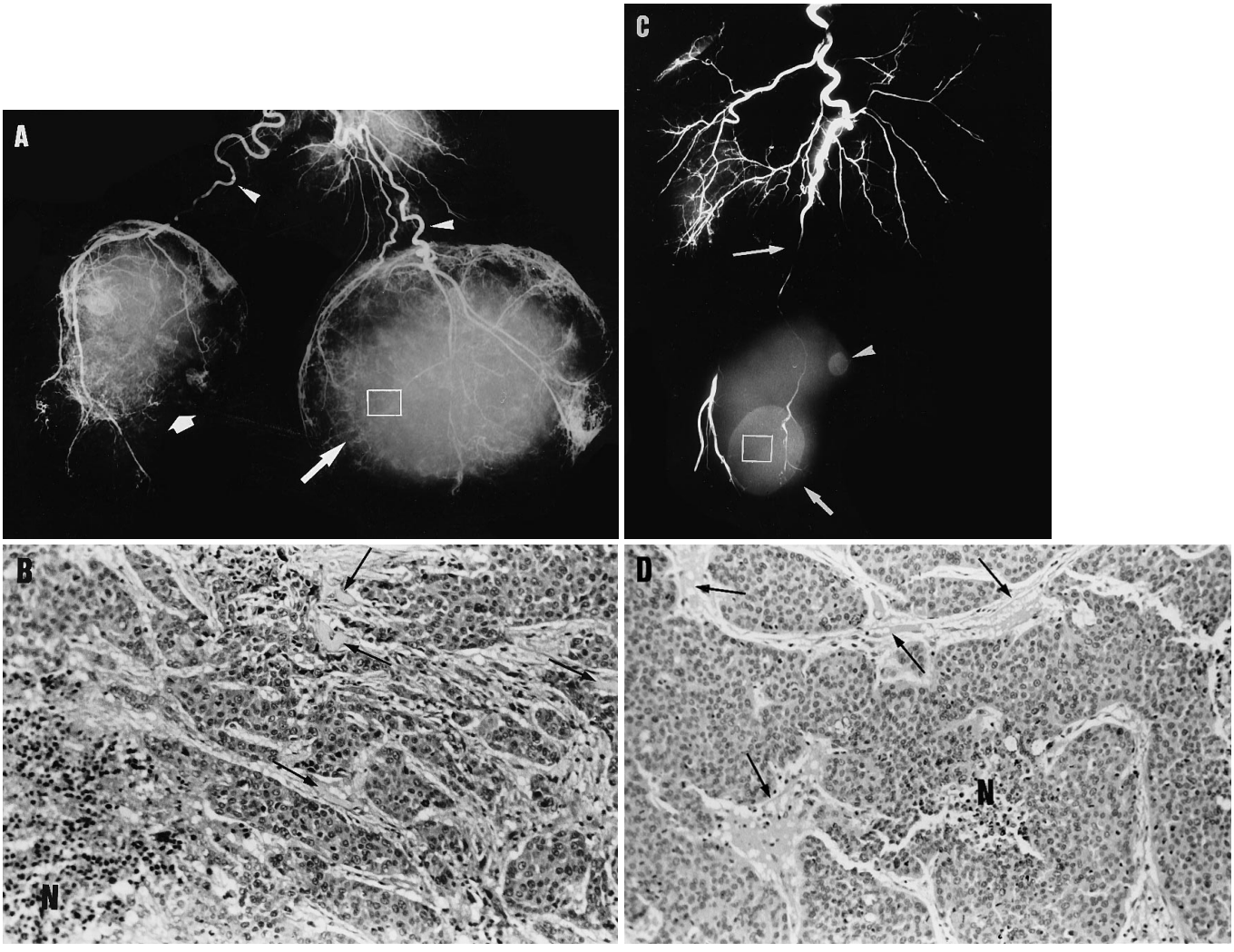

Fig. 3. Microangiographic and histopathological comparisons between VX2 tumors **A,B** without RF ablation and **C,D** shortly after RF ablation. **A** Microangiogram of the liver from a rabbit of sham-operated group shows that two hypervascularized VX2 tumors have occupied almost the entire right *(short arrow)* and left *(long arrow)* liver lobes 7 weeks after tumor implantation. *Arrowheads* indicate hypertrophic and tortuous feeding arteries. The *square* approximates where the histologic sample was taken. **B** Light-microscopic view from the same rabbit as in **A** displays the amorphous characters of this highly malignant carcinoma including nests of viable tumor cells, spontaneous necrosis *(N)*, and multiple intratumoral blood vessels *(arrows)* which are filled with injected barium (yellow-greenish tiny particles as viewed under microscope). (Hematoxylin and eosin staining, original magnification × 200). **C** Microangiogram of the liver from a rabbit immediately after RF ablation shows that the main tumor *(short arrow)* and a satellite metastasis *(arrowhead)*, as well as the surrounding normal liver tissue, are well encompassed in the range of ablation. The tumoral feeding artery *(long arrow)* is almost discontinued with the residual intra- and peritumoral blood vessels, which are overwhelmingly destroyed. The *square* indicates where the microscopic view was taken. **D** Light-microscopic view of the VX2 tumor from the same rabbit as in **C** displays an almost identical appearance to viable tumor tissue **(B)**, despite complete tumor ablation, which is known as the "ghost" phenomenon. The nuclei and cytoplasm are only slightly less colored with hematoxylin and eosin staining without any obvious sign of tissue destruction. However, instead of barium particles as seen with the viable tumor **(B)**, only coagulated blood or plasma with heat-induced evaporation air bubbles are seen in the cavities of intratumoral blood vessels *(arrows)*. Although indirect, this sign in combination with microangiographic findings facilitates discrimination between viable and acutely ablated tumoral tissues. *N* stands for spontaneous tumor necrosis which occurred before RF ablation (hematoxylin and eosin staining, original magnification × 200)

sion shortly after RFA, except the small vacuolated and/or charred area around the needle track, the ablated lesion is composed mainly of a large paled area of coagulation necrosis and demarcated with a thin dark-brown layer corresponding to the congestion. Microscopically, typical coagulation necrosis appeared only several weeks after RFA. Peripheral inflammatory tissue reaction was followed by granulation and scar tissue formation (Fig. 2G, H). All autolytic and subsequent repairing changes developed from the periphery or from where there were remaining intralesional blood vessels (Fig. 2G).

In control groups, nests of viable tumoral cells coexisted with foci of spontaneous tumor necrosis especially in the central area (Fig. 3B). This type of necrosis was characterized with pyknotic, karyorrhectic nuclei, and clasmatosis (Fig. 3B). Abundant intratumoral vessels were filled with injected barium (Fig. 3A, B).

However, from hours to days after RFA therapy, the ablated tissues, including tumors and adjacent liver, appeared almost unchanged microscopically (Fig. 3D). Although being not yet widely known, this "ghost" phenomenon occurs following most of the thermotherapies as a consequence of sudden tissue coagulation or fixation. At the hematoxylin–eosin staining, the ablated

nonviable tissues (Fig. 3D) were stained only slightly lighter than viable tissues (Fig. 3B). The absence of barium filling in intralesional vessels was, however, indirect evidence of tissue death (Fig. 3D). Histologically, it was easier to identify spontaneous tumor necrosis than to distinguish viable from freshly ablated nonviable "ghost" tissues (Fig. 3B, D).

Discussion

In RFA, an alternating radio-frequency current flows from a metal electrode to the tissue. Ionic agitation around the electrode causes frictional heating and thermal ablation of the tissue. However, the lesion size is limited with conventional RFA technique due to a sudden impedance rise around the electrode and a cease of RF energy delivery as a result of tissue desiccation. With the present modified technique, interstitial infusion of hypertonic saline via the hollow needle serves as a "liquid electrode." This improves the conductivity of electrode–tissue interface by filling the gap with abundant conductive ions and prevents overheating and impedance rise. The effective surface area at the electrode tip is enlarged and the spread of RF energy into surrounding tissue is therefore improved, resulting in increased lesion size [21, 22].

VX_2 carcinoma is a rabbit tumor of epithelial origin, derived from a virus-induced papilloma [24]. This tumor line is extremely malignant and can be allogeneously transplanted almost anywhere in rabbits [25]. Liver implantation of VX2 tumors has been extensively used in imaging studies to simulate human hepatic metastasis, but only in few studies for tumor therapy. The discouraging therapeutic effects in previous studies can be partially attributed to the aggressiveness of this tumor line and to the disseminative tendency with inoculation of VX2 tumor cell suspension [26]. Therefore, this tumor model has been generally considered as incurable and useful mainly for studies in tumor detection. As demonstrated in the present study (Table 1), a substantial percentage of rabbits with VX2 liver tumors were radically treated with current RFA therapy, although the overall tumor size of RF treated group prior to therapy was basically the same as that of control groups. The eradication of VX2 tumors in this study was either absolutely proved by follow-up longer than 6 months after tumor implantation (any tumor relapse would cause animal death within this period) or relatively supported by MRI, microangiographic, and histologic findings. To our knowledge, this is the first report in which a large percentage of liver VX2 tumors were eradicated. This encouraging result can be attributable to at least three reasons. Firstly, as shown in the ex vivo study [22], the applied RF ablation technique was able to induce a tissue necrosis > 3 cm in diameter, which encompasses both the tumor and a safety margin of surrounding liver parenchyma. Secondly, in this study, fragments of VX2 tumor tissue instead of tumor cell suspension were implanted. This method induces a solitary mass and largely avoids simultaneous malignant dissemination via blood and/or lymph circulation as seen with VX2 suspension inoculation [26]. Lastly, in the present study, the RFA was performed under laparotomy, which enabled us to accurately target the tumor, control the lesion size, and avoid injury to the adjacent organs.

Besides percutaneous procedure, RFA can be performed under mini-laparotomy or laparoscopy. Such open RFA procedures can be advantageous since the hepatic inflow can be temporarily obstructed, which may minimize the cooling effect caused by blood flow [20, 27, 28, 29].

The characteristic MRI appearances of liver tumor and ablated lesion, including the tumor and surrounding liver, can be utilized for imaging guidance of RFA procedure, therapeutic assessment, and follow-up. The hyperintense and hypointense signals of the lesions on in vivo T1- and T2-weighted MR images early after RFA confirm the previous ex vivo findings [22]. At late phase, unabsorbed necrosis and scarring tissue featured, respectively, hyperintense and hypointense signals on T1-weighted MRI, whereas an opposite contrast occurred with these two components on T2-weighted MRI (Fig. 2C, D). Tumor relapse and lung metastasis can be reliably detected with MRI scanning.

VX2 tumors are known to be hypervascularized. The presence of an avascular region on microangiogram presents a typical change after RFA. This phenomenon suggests that destruction of tumoral vessels is one of the important factors associated with tissue death in this therapy.

At histology, VX2 carcinoma is frequently accompanied with spontaneous necrosis which can be easily recognized (Fig. 3B, D) and should not be mistaken as therapeutic necrosis caused by RFA. But the suddenly ablated tissues appeared almost intact and constitute so-called ghost phenomenon, which should be more carefully differentiated from unablated viable tissues (compare Fig. 3B, D). Failure in this respect may cause misevaluation of the therapy. The ghost phenomenon is normally found in the large area of the lesion peripheral to the central electrode track, which is composed of charred and vacuolated tissues. Sudden tissue coagulation may prevent enzyme release from intracellular lysosomes and postpone subsequent cellular autolysis. On the other hand, as a result of destroyed intratumoral vessels, inflammatory cells, such as macrophages and polymorphonuclear leukocytes, cannot infiltrate into the region and participate in tissue autolysis. These are proposed mechanisms for the observed ghost phenomenon.

Despite a high cure rate of VX2 tumors after RFA in this study, tumor recurrence in the liver and metastasis to the lungs did occur in some animals. Although there was no statistical difference in lung metastasis between saline-infusion-only and untreated groups, theoretically, infusion of a certain amount of saline into the tumor may increase the static interstitial pressure which in turn may force individual tumor cells to migrate to adjacent or remote areas. Intercellular junction of malignant tumor is known to be much looser than that of normal

tissue [30], which is one of the elements of metastatic tendency. This danger can be lowered by decreasing the amount of saline infusion while further increasing its concentration and by temporarily obstructing hepatic inflow in order to minimize the risk of tumor cell migration during the therapy. Further investigation is warranted to address this issue.

In conclusion, the present animal experiment has demonstrated that radical treatment of liver malignancy is possible with current hypertonic saline-infusion-mediated RFA. Further experiments are needed to optimize a technique that can be eventually used for clinical oncology.

Acknowledgement. The authors are grateful to P. Mulier of Medtronic Inc., and to M.F. Hoey of University of Minnesota for providing the RF generator, and for our informative discussions.

References

1. Farmer DG, Rosove MH, Shaked A, Busuttil RW (1994) Current treatment modalities for hepatocellular carcinoma. Ann Surg 219: 236–247
2. Venook AP (1994) Treatment of hepatocellular carcinoma: too many options? J Clin Oncol 12: 1323–1234
3. Simonetti RG, Liberati A, Angiolini C, Pagliaro L (1997) Treatment of hepatocellular carcinoma: a systematic review of randomized controlled trials. Ann Oncol 8: 117–136
4. Adam R, Akpinar E, Johann M et al. (1997) Place of cryosurgery in the treatment of malignant liver tumors. Ann Surg 225: 39–50
5. Lencioni R, Pinto F, Armillotta N et al. (1997) Long-term results of percutaneous ethanol injection therapy for hepatocellular carcinoma in cirrhosis: a European experience. Eur Radiol 7: 514–519
6. Orlando A, Cottone M, Virdone R et al. (1997) Treatment of small hepatocellular carcinoma associated with cirrhosis by percutaneous ethanol injection. A trial with a comparison group. Scand J Gastroenterol 32: 598–603
7. Yamanaka N, Tanaka T, Oriyama T et al. (1996) Microwave coagulonecrotic therapy for hepatocellular carcinoma. World J Surg 20: 1076–1081
8. Matsukawa T, Yamashita Y, Arakawa A et al. (1997) Percutaneous microwave coagulation therapy in liver tumors. A 3-year experience. Acta Radiol 38: 410–415
9. Vogl TJ, Mack MG, Straub R et al. (1997) Magnetic resonance imaging-guided abdominal interventional radiology: laser-induced thermotherapy of liver metastases. Endoscopy 29: 577–583
10. Hill CR, ter Haar GR (1995) Review article: high intensity focused ultrasound: potential for cancer treatment. Br J Radiol 68: 1296–1303
11. Prat F, Centarti M, Sibille A et al. (1995) Extracorporeal high-intensity focused ultrasound for VX2 liver tumors in the rabbit. Hepatology 21: 832–836
12. Rossi S, Stasi M di, Buscarini E et al. (1996) Percutaneous RF interstitial thermal ablation in the treatment of hepatic cancer. Am J Roentgenol 167: 759–768
13. Livraghi T, Goldberg SN, Monti F et al. (1997) Saline-enhanced radio-frequency tissue ablation in the treatment of liver metastasis. Radiology 202: 205–210
14. Solbiati L, Goldberg SN, Ierace T et al. (1997) Hepatic metastases: percutaneous radio-frequency ablation with cooled-tip electrodes. Radiology 205: 367–373
15. Lorentzen T (1996) A cooled needle electrode for radiofrequency tissue ablation: thermodynamic aspects of improved performance compared with conventional needle design. Acad Radiol 3: 556–563
16. Goldberg SN, Gazelle GS, Solbiati L et al. (1996) Radiofrequency tissue ablation: increased lesion diameter with a perfusion electrode. Acad Radiol 3: 636–644
17. Lencioni R, Goletti O, Armillotta N et al. (1998) Radio-frequency thermal ablation of liver metastases with a cooled-tip electrode needle: results of a pilot clinical trial. Eur Radiol 8: 1205–1211
18. McGahan JP, Gu WZ, Brock J et al. (1996) Hepatic ablation using bipolar radiofrequency electrocautery. Acad Radiol 3: 418–422
19. Rossi S, Buscarini E, Garbagnati F et al. (1998) Percutaneous treatment of small hepatic tumors by an expandable RF needle electrode. Am J Roentgenol 170: 1015–1022
20. Patterson EJ, Scudamore CH, Owen DA et al. (1998) RF ablation of porcine liver in vivo: effects of blood flow and treatment time on lesion size. Ann Surg 227: 559–565
21. Hoey MF, Mulier PM, Shake JG (1995) Intramural ablation using radiofrequency energy via screw-tip catheter and saline electrode. PACE 18: 917
22. Miao Y, Ni Y, Mulier S et al. (1997) Ex vivo experiment on radio-frequency liver ablation with saline infusion through a screw-tip cannulated electrode. J Surg Res 71: 19–24
23. Yang R, Rescorla FJ, Reilly CR et al. (1992) A reproducible rat liver cancer model for experimental therapy: introducing a technique of intrahepatic tumor implantation. J Surg Res 52: 193–198
24. Kidd JG, Rous P (1940) A transplantable rabbit carcinoma originating in a virus-induced papilloma and containing the virus in masked or altered form. J Exp Med 71: 813–838
25. Yamada K, Jinbo T, Miyahara K et al. (1996) Contrast-enhanced MRI with gadodiamide injection in rabbit carcinoma models. J Vet Med Sci 58: 389–396
26. Nishizaki T, Matsumata T, Kanematsu T et al. (1990) Surgical manipulation of VX2 carcinoma in the rabbit liver evokes enhancement of metastasis. J Surg Res 49: 92–97
27. Kolios MC, Sherar MD, Hunt JW (1995) Large blood vessel cooling in heated tissues: a numerical study. Phys Med Biol 40: 477–494
28. Sturesson C, Liu DL, Stenram U, Andersson-Engels S (1997) Hepatic inflow occlusion increases the efficacy of interstitial laser-induced thermotherapy in rat. J Surg Res 71: 67–72
29. Goldberg SN, Hahn PF, Tanabe KK et al. (1998) Percutaneous RF tissue ablation: dose perfusion-mediated tissue cooling limit coagulation necrosis? J Vasc Interv Radiol 9: 101–111
30. Poste G, Fidler IJ (1980) The pathogenesis of cancer metastasis. Nature 283: 139–146